Here, γ is the specific acoustic radiation admittance of the continuum, $\gamma_f = 1/\rho_f c_f$. The difference of these intensities is the intensity of the acoustic energy absorbed in the cavitation region. Thus, when compared with the theoretical results of the given model, the experimental values of γ for each oscillatory velocity obtained in [26] were recalculated by the following expression:

$$\frac{I_a}{p_0} = (\gamma - \gamma_f) p_0 \tag{15}$$

In representing the data of the work [26], the values of $(v_t)_{rms}$ were determined directly from the experimental plots of this work at the point of characteristic inflection.

2.5. Experimental Setup

To measure the acoustic energy absorbed in a cavitating liquid at increased static pressure p_0, an acoustic calorimeter described in section 3.2.3 of this book was used. Static pressure in the calorimeter was produced with compressed nitrogen. Settled tap water at 20^0 C was used. The static pressure, p_0, varied in the range 1.0 – 5.0 bar; the water density, $\rho_f = 998$ kg/m^3 sound velocity in the water, $c_f = 1500$ m/s; the volume of air dissolved in unit mass of water, $\eta_0 = 2.2 \cdot 10^{-5}$ m^3/kg. Each experimental point shown on the plots was obtained as a mean value of 10 measurements.

2.6. Experimental Results

Experimental data for small oscillatory velocities of an acoustic radiator, v_t and different static pressures, p_0, are shown in Figure 5. The values of v_t used in the treatment of these experimental data were calculated from the expression $(v_t)_{rms} = 0.707 p_0/\rho_f c_f$ for different static pressures. Also shown in this figure are the experimental data from [26] for ultrasound frequencies of 19 and 28 kHz, closest to the frequency 17.8 kHz used in the present work, which are interpreted by equation (15). The values of the cavitation threshold obtained from the corresponding plots of [26] for both frequencies $(v_t)_{rms} = 0.08$ m/s. Figure 5 also shows the theoretical lines calculated from equations

(11) and (12), which are represented by the solid and the dotted lines, respectively.

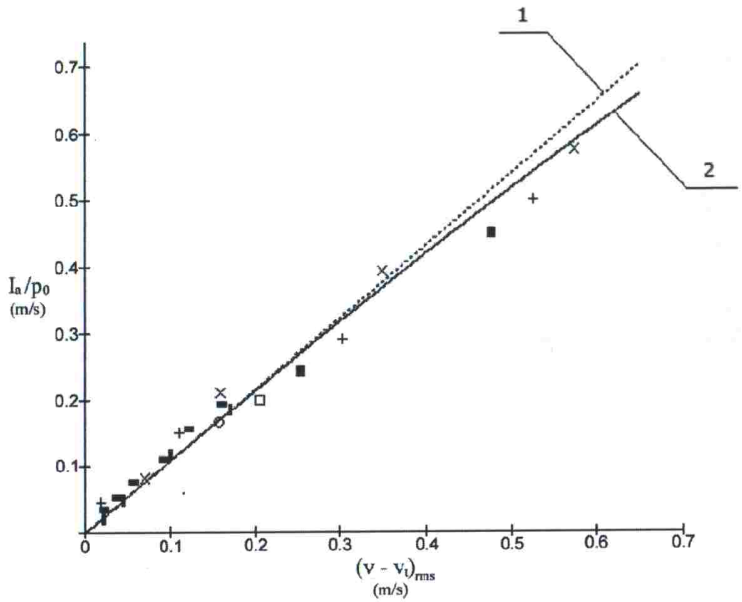

Figure 5. Intensity of acoustic energy absorbed in water at cavitation is shown as a function of the excessive oscillatory velocity of an acoustic radiator for pressures of × - 1 bar, + - 2 bar, ■ - 3 bar, □ - 4 bar, ○ - 5 bar, at frequencies of ▌- 28 kHz and ▬ - 19 kHz from the work [26]. Line 1 is plotted from equation (12); line 2 is plotted from equation (11).

A good agreement between the theoretical lines themselves and the experimental data with these lines at small values of v can be clearly seen. With increasing $(v\text{-}v_l)_{rms} > 0.2$ *m/s*, the experimental points diverge from the straight line plotted from equation (12) and approach the line plotted from equation (11).

Figure 6 shows the experimental results for all oscillatory velocities of the acoustic radiator, v, which were used in the experiments at normal static pressure, $p_0 = 1$ bar. Also shown in this figure are the theoretical lines plotted from equations (11) and (14). From Figure 6 it is seen that at intermediate values of v the experimental points are located near practically coincident lines plotted from equations (11) and (14), which are represented by the dotted and solid lines, respectively.

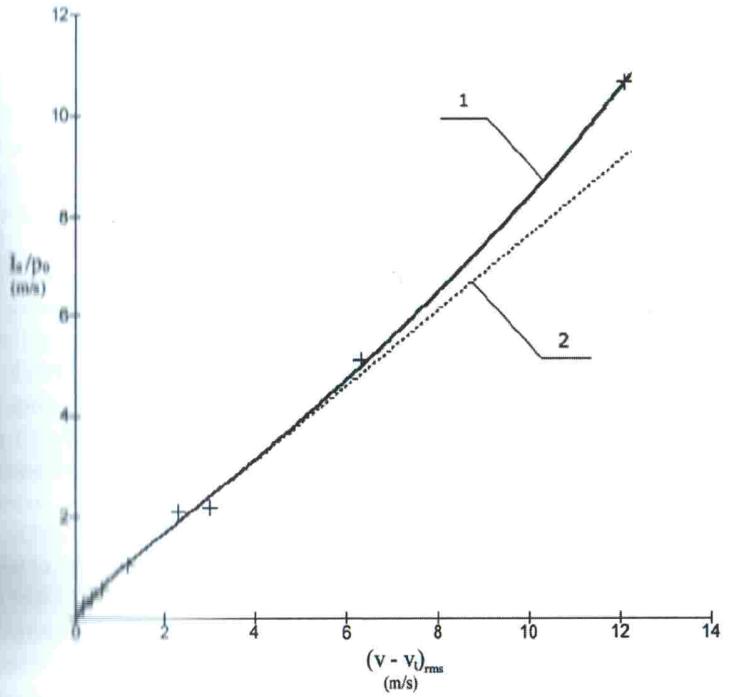

Figure 6. Intensity of acoustic energy absorbed in water at cavitation is shown as a function of the excessive oscillatory velocity of an acoustic radiator. Line 1 is plotted from equation (14); line 2 is plotted from equation (11).

At high oscillatory velocities, $(v\text{-}v_l)_{rms} > 3$ m/s, the specified theoretical relationships diverge, and the experimental points are located according to a more general relationship (14) at $\alpha_h = 0.4$. It can be seen that the theoretical and the experimental data are in good agreement up to the highest values of the oscillatory velocity, v.

A spread of the experimental points on the curve in Figure 6 in the region 2 m/s < $(v\text{-}v_l)_{rms} < 3$ m/s is also observed. Here, the beginning of the divergence of the theoretical curves 1 and 2 is observed as well. These phenomena are, apparently, associated with the establishment of the supersonic regime of the SW movement and a considerable decrease in the gas pressure in the bubbles. The indication of the possibility of the supersonic regime of radiation at acoustic cavitation was first made in the work [27]. The phenomenon itself was called the second threshold of acoustic cavitation. The region located over the second threshold at $(v\text{-}v_l)_{rms}$

> 3 m/s was called the region of acoustic supercavitation. The closest related known phenomenon is called hydrodynamic supercavitation and is described, for example, in [28].

Since, as the stated theory assumes, at supercavitation the spherical shock wave is not formed in the gas inside the bubbles, at oscillatory velocities $(v\text{-}v_l)_{rms} > 3$ m/s the characteristic changes of the secondary effects of cavitation, which are used in the sonochemical technology, must be observed.

An experimental verification of this effect was conducted by observing the cavitation-induced ultrasonic dispersion of solid particles. During the experimental setup, it was assumed that the transition to the supercavitation regime should in some way be reflected in the manner in which the dispersion occurs. The experimental study was conducted during the ultrasonic dispersion of graphite particles with the initial size 200-250 μ in settled tap water under normal conditions. To avoid any possible influence of the reactor geometry on the results of the measurements, the acoustic calorimeter described in section 3.2.3 was used as an apparatus for dispersing. For the analysis of the relative transparency of the obtained dispersions, the degree of the light absorption (at the wavelength of 420 nm) in them was measured using a photo-colorimeter. From the measurement results presented in Figure 7 in relative units, it can be seen that the obtained curve reaches a maximum and then discontinues at 2.5 m/s $< (v\text{-}v_l)_{rms} <$ 3 m/s. A subsequent smooth rise of this curve in the supercavitation region is also observed, which is most likely associated with the intense acoustic streaming, rather than with the effect of cavitation itself.

It appears that it is in the acoustic supercavitation region where the achievement of the highest possible temperatures during the compression of the rarefied gas inside the bubble oscillating as a Rayleigh cavity can be expected. Pressure at the bubble wall at the moment of focusing theoretically approaches infinitely high values because the gas compression is exerted by the moving dense bubble wall acting as a spherical plunger, rather than by a spherical acoustic wave [19]. In the same region, the highest intensities of the cavitation-induced sonochemical processes occurring at high temperatures may be observed. At the same time, processes connected with erosion, dispersion of solids and the like can be inhibited in the supercavitation region.

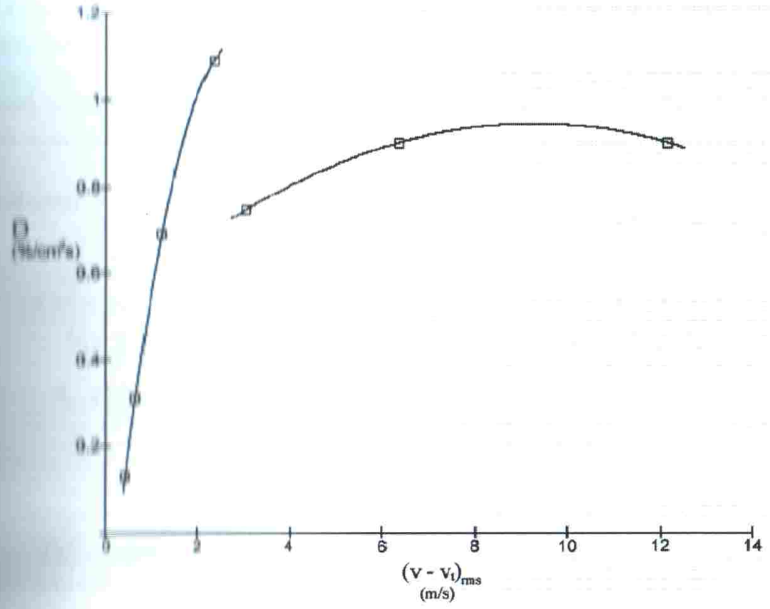

Figure 7. Dispersing effect of acoustic cavitation (dispersion of graphite powder in water) determined by the degree of the 420 nm wavelength light absorption is illustrated as a function of the excessive oscillatory velocity of an acoustic radiator.

2.7. Section Conclusions

The proposed shock-wave model of acoustic cavitation reflects real events occurring in water at cavitation since calculations based on the equations that follow from the model are in good agreement with the results of the experiments. The presented experimental data extend to the region of super-high oscillatory velocities of an acoustic radiator and agree well with the theoretical model. The model makes it possible to obtain the resulting equation for the calculations of the energy absorbed by liquids during cavitation without having to consider in detail all the complex processes of the absorption of the acoustic energy, which are connected with the nonlinear oscillations of the gas bubbles during their collapse.

Within the framework of this model, the existence of a transition from the subsonic regime of acoustic cavitation to the supersonic regime is

predicted. The possibility of a change in the character of the oscillations of a cavitation bubble at high values of v is theoretically shown. The conducted experimental studies confirm such a possibility.

As will be shown below, simple algebraic expressions that follow from the proposed model can be used in practical engineering calculations for designing powerful ultrasonic horns for sonochemical reactors.